
Being the Fire A CNN-Based Reinforcement Learning Method to Learn How Fires Behave Beyond the Limits of Physics-Based Empirical Models

William L. Ross

Department of Earth, Energy, and Environmental Sciences
Stanford University
Stanford, CA 94305
wlross@stanford.edu

Abstract

1 Wildland fires pose an increasing threat in light of anthropogenic climate change.
2 Fire-spread models play an underpinning role in many areas of research across this
3 domain, from emergency evacuation to insurance analysis. We study paths towards
4 advancing such models through deep reinforcement learning. Aggregating 21 fire
5 perimeters from the Western United States in 2017, we construct 11-layer raster
6 images representing the state of the fire area. A convolution neural network based
7 agent is trained offline on one million sub-images to create a generalizable baseline
8 for predicting the best action - burn or not burn - given the then-current state on
9 a particular fire edge. A series of online, TD(0) Monte Carlo Q-Learning based
10 improvements are made with final evaluation conducted on a subset of holdout fire
11 perimeters. We examine the performance of the learned agent/model against the
12 FARSITE fire-spread model. We also make available a novel data set and propose
13 more informative evaluation metrics for future progress.

14 **1 Introduction**

15 The performance of fire-spread models, which aim to predict the spatial spreading process of an active
16 fire across a given area, is important to protecting our communities from wildfire. Most contemporary
17 fire spread models can be traced back to a single 1972 paper – *A Mathematical Model for Predicting*
18 *Fire Spread in Wildland Fuels* – authored by Richard Rothermel [1]. While Wells (2008) points out
19 that the Rothermel Model's empirical, physically-informed approach is "still running like a champ",
20 many experts recognize that the model is now being asked to do things it was never meant to do [2].

21 The last decade has seen marked progress in the fields of deep learning and reinforcement learning
22 and has spurred a new era for machine learning and artificial intelligence [3,4]. In the field of
23 deep learning, convolutional neural networks exhibit unique predictive ability in image recognition
24 tasks, including those that use remote sensing [5,6]. Deep reinforcement learning, meanwhile, has
25 demonstrated the ability to solve complex optimization problems dynamically and over time in the
26 presence of uncertainty [7].

27 Combining these techniques, there is initial evidence to suggest that deep reinforcement learning can
28 be used to learn wildfire dynamic models from historic observations and remote sensing data. We
29 extend the work of Subramanian and Crowley – *Using Spatial RL to Build Forest Wildfire Dynamics*
30 *Models From Satellite Images* – in hopes of unifying the latest remote sensing data, machine learning
31 algorithms, and physical techniques to advance fire spread modeling [8].

32 **2 Review of Literature**

33 **2.1 Fire-Spread Modeling and Prediction**

34 The vast majority of today's fire-spread models represent small changes to individual characteristics
35 within the framework provided by Rothermel. Models such as FARSITE and BehavePlus are
36 widely adopted in commercial and government work today but typically focus on improving select
37 parameters, with incremental progress in each new generation [9,10]. But the reality in the words of
38 Rothermel pupil Brett Butler, is that "(these models describe) very well a fire burning in a field of
39 wheat. As you get further away from that uniformity, the less accurate (they) become [11]."

40 Among the most meaningful areas of such progress has been the improvement of topographic wind
41 speed modeling. Because most wildfires do not burn in a field of wheat, understanding how wind
42 changes speed in complex topography is important to assessing speed and direction of fire spread.
43 Wagenbrenner et al. (2016) make use of physical conservation of mass and momentum to downscale
44 surface wind predictions or measurements in complex terrains [12]. While such solvers are intended to
45 improve the Rothermel framework, they yield equally useful inputs for machine learned approaches.

46 **2.2 Machine Learning and Remote Sensing in Fire-Spread Models**

47 The science of remote sensing has advanced as the resolution, coverage, and frequency of such data
48 improves [13]. Government funded projects such as Landsat 8 (2013) and Sentinel 1-A/B (2014-16)
49 provide high resolution (20-30m) data at a consistent frequency [14,15]. Private companies such as
50 Planet provide further coverage through projects like RapidEye (5m) and Planetscope (3m), both of
51 which provide data from much of the planet on a daily frequency or better.

52 Such data has opened the door for the use of machine learning in various applications in wildfire. For
53 example, Zhang et al. (2011) provide a hybrid model that makes use of satellite imagery and is now
54 used in the Canadian Forest Fire Weather Index (FWI) [16]. The use of sequential models in the form
55 of markov decision processes (MDP) offers another path forward particularly relevant to fire-spread
56 models. In Subramanian and Crowley (2019), a number of methods including Q-Learning, monte
57 carlo tree search, and deep reinforcement learning are identified as promising opportunities.

58 **3 Problem Formulation/Methods**

59 We evaluate the spread of wildfire in a grid-based 30m resolution environment on the USGS Contiguous
60 Albers Equal Area Conic coordinate reference system as an MDP S, A, P, R . Our continuous
61 state space, S , represents the then-current state of a given cell on the fire edge as represented by an
62 11x3x3 raster of that cell and all adjacent cells. 10 layers represent constants over the observation
63 period and 1 layer represents the dynamic condition of where the fire has or has not spread at a given
64 time step T . Our binary action space, A , is a simple burn, not burn choice for each unburned grid
65 cell on the fire edge at each time step. Our transition probability P is represented as a convolutional
66 neural network (CNN) and estimates the likelihood that a burn or not burn action will maximize our
67 reward R - the negative binary cross-entropy loss of the CNN at each time step.

68 All code and data used for model/agent training and analysis are publicly available for reuse: github.com/wlross/Being_The_Fire_Final.

70 **3.1 Data Acquisition and Processing**

71 Critical to this approach is the state space as represented by historical data from each fire perimeter. A
72 total of 42 fire perimeters representing a T=0 and T=Final perimeter for each of 21 fires (see Appendix
73 A) from the 2017 wildfire season in the Western United States were collected via GeoMAC [17].
74 Fires were manually curated to ensure consistent measurement methodologies and a geographical,
75 topographical, and fuel load distribution consistent with the full set of 7418 GeoMAC perimeters
76 from the 2017 fire season.

77 For each fire boundary, a bounding-box representing the edges at T=Final was created and gridded
78 into 30m cells. For each grid point, 10 data characteristics were gathered from several sources
79 including: *Planet 5m Resolution RapidEye Program* - Red (1), Green (2), Blue (3), Red Edge (4), and

80 Near Infrared (5) Imagery, *US Geological Survey* - 30m Resolution Topography, *National Weather*
 81 *Service* - Average Wind Speed and Direction (7,8) and Maximum Wind Speed and Direction (9,10)
 82 [18,19,20]. All values were imputed to the final 30m resolution grid using mean or nearest neighbor
 83 approaches as appropriate.

84 **3.2 Training and Evaluation**

85 In order to train our agent, two distinct phases of model training were used. The initial offline training
 86 approach was introduced to increase the generalizability of the online model. The offline environment
 87 was also used for experimentation and hyper-parameter tuning as detailed in Appendix B. The model
 88 architecture used in both offline and online training is visualized as follows:

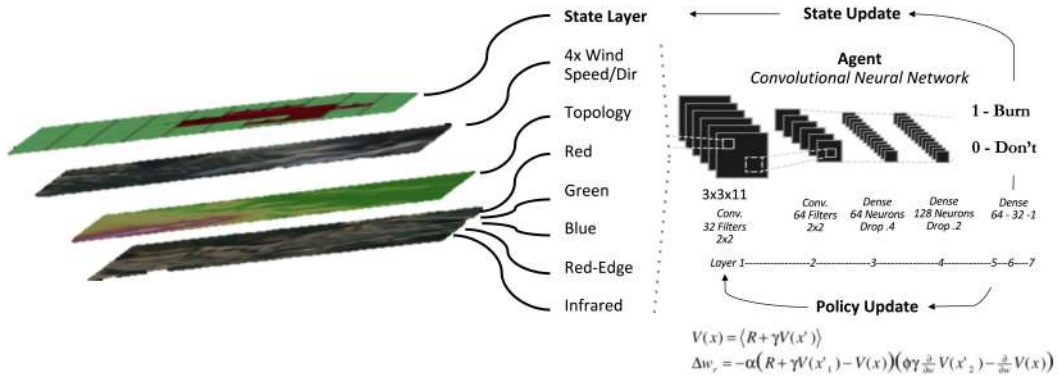


Figure 1: Model architecture for convolutional neural network and TD(0) Monte Carlo Q-Learning

89 For online training, weights from offline training were transferred and additional training was
 90 conducted using a TD(0) Monte Carlo Q-Learning algorithm. The reinforcement learning aspect of
 91 this approach was consistent with the work of Subramanian and Crowley with the primary difference
 92 being the CNN representation of the agent and the use of more, higher resolution data layers.
 93 Results for final evaluation were generated using the trained agent on the four holdout fires. In
 94 parallel, the FlamMap 6 package was used to generate benchmark data via the FARSITE model using
 95 default parameters and landscape files available via the LANDFIRE program [21].

96 **4 Analysis of Results**

97 **4.1 Quantitative Model Performance**

98 Quantitative model performance was measured using the Weighted Average F-1 Score as the primary
 99 metric, recognizing that accuracy measures may overstate performance of "under-burn" or "over-
 100 burn" models depending on the denominator used. For this research, all grid squares within the
 101 bounding box that were not already ignited at T=0 were used for analysis in order to fairly weight both
 102 "under-burn" and "over-burn" behaviors. Results were not compared to Subramanian and Crowley
 103 as the accuracy metrics presented did not provide a reasonable means for direct comparison and
 104 reproducing this work was challenging.

Table 1: Reinforcement Learning (RL) and FARSITE (FS) Model Performance

Fire Name	Reinforcement Learning			FARSITE Benchmark		
	Precision	Recall	F-1	Precision	Recall	F-1
Buck	.82	.78	.74	.64	.45	.44
Highline	.77	.69	.59	.62	.43	.39
Pinal	.84	.84	.81	.84	.20	.08
Sulfur	.78	.72	.64	.79	.73	.74

Weighted average 0s and 1s in t=0 unburned sample area

105 The RL-Model outperformed the FARSITE model on 3/4 test fires, though both had low F-1 scores.
106 In general, this was due to "under-burn" by the RL Model (low class 1 recall) and "over-burn" by
107 the FARSITE model (low class 0 recall). Both methods performed similarly on class 0 precision but
108 the RL model significantly outperformed the FARSITE model on class 1 precision, providing some
109 evidence of a better "fit" by the RL model.

110 4.2 Qualitative Model Performance

111 Given the relatively low F-1 scores exhibited by both the RL and FARSITE model, a smoothing func-
112 tion was applied to the fire perimeter so that the final fire boundaries could be inspected qualitatively.
113 This is consistent with expected use in the field - see Appendix C.

114 In both cases, models appeared to be performing in ways consistent with our understanding of
115 physical fire spread - burn was driven by wind direction, slope, and vegetation and obstructed by
116 roads, rivers, and lakes. A visual inspection of the fire spread patterns provides some indication of
117 superior performance by the RL model. For instance, the fire road present in the Highline fire and the
118 river present in the Pinal both seem to have influenced a closer fit to the ground truth data for the RL
119 model when compared to FARSITE, which crossed these boundaries easily - see Figure 2.

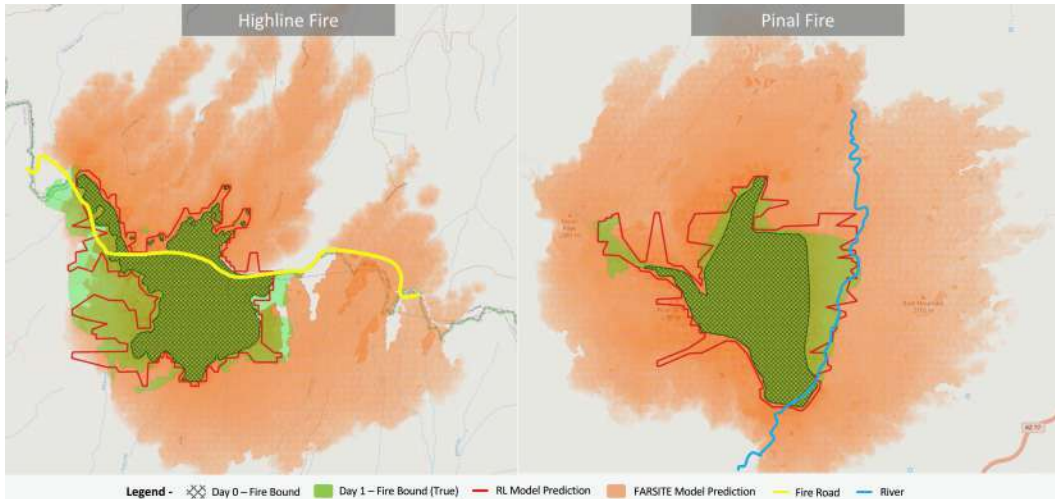


Figure 2: RL + FARSITE Models of Highline and Pinal Fires from Test Set

120 5 Discussion

121 The reality of fire spread models is that they are attempting to model highly stochastic physical
122 processes. But given such models serve as a critical building block for climate adaptation to wildland
123 fires, progress is important. When compared to existing methods like FARSITE, the results of this
124 work support continued exploration of deep reinforcement learning approaches in this domain.

125 The CNN-based RL methods proposed in this paper have the advantage of tailwinds in both machine
126 learning research and remote sensing data availability. One challenge to progress, however, is the
127 availability of remote sensing data at high resolution and high frequency. Notably, these dependencies
128 are often also present (and sometimes less obvious) when working with physical models.

129 Another source of challenge in this direction is the lack of standardization. Metrics like accuracy that
130 have been previously reported lack sufficient context for determining model performance. The use
131 of metrics like the weighted average F-1 score, which factors in both "under-burn" and "over-burn",
132 alongside qualitative assessments provide an opportunity to establish new benchmarks.

133 It is clear that reinforcement learning methods for fire-spread modeling are not without their chal-
134 lenges. Still, this work demonstrates the potential for learned methods to, over time, add value to
135 progress in fire-spread modeling.

136 **References**

- 137 [1] Rothermel, Richard C. A mathematical model for predicting fire spread in wildland fuels. Vol. 115.
138 Intermountain Forest Range Experiment Station, Forest Service, US Department of Agriculture, 1972.
- 139 [2] Wells, Gail. "The Rothermel Fire-Spread Model: still running like a champ." (2008).
- 140 [3] LeCun, Yann, Yoshua Bengio, and Geoffrey Hinton. "Deep learning." *nature* 521.7553 (2015): 436-444.
- 141 [4] Watkins, Christopher JCH, and Peter Dayan. "Q-learning." *Machine learning* 8.3-4 (1992): 279-292.
- 142 [5] Krizhevsky, Alex, Ilya Sutskever, and Geoffrey E. Hinton. "Imagenet classification with deep convolutional
143 neural networks." *Advances in neural information processing systems* 25 (2012): 1097-1105.
- 144 [6] Zhang, Wei, Ping Tang, and Lijun Zhao. "Remote sensing image scene classification using CNN-CapsNet."
145 *Remote Sensing* 11.5 (2019): 494.
- 146 [7] Mnih, Volodymyr, et al. "Playing atari with deep reinforcement learning." *arXiv preprint arXiv:1312.5602*
147 (2013).
- 148 [8] Subramanian, Sriram Ganapathi, and Mark Crowley. "Learning forest wildfire dynamics from satellite
149 images using reinforcement learning." *Conference on reinforcement learning and decision making*. Ann Arbor
150 MI, 2017.
- 151 [9] Finney, Mark A. *FARSITE, Fire Area Simulator—model development and evaluation*. No. 4. US Department
152 of Agriculture, Forest Service, Rocky Mountain Research Station, 1998.
- 153 [10] Andrews, Patricia L. "BehavePlus fire modeling system: past, present, and future." In: *Proceedings of 7th*
154 *Symposium on Fire and Forest Meteorology*; 23-25 October 2007, Bar Harbor, Maine. Boston, MA: American
155 Meteorological Society. 13 p.. 2007.
- 156 [11] Gabbert, Bill. "Throwback Thursday: The origin of the model for predicting the spread of wildland fires."
157 In: *Wildfire Today*, June 2018.
- 158 [12] Wagenbrenner, Natalie S., et al. "Downscaling surface wind predictions from numerical weather prediction
159 models in complex terrain with WindNinja." *Atmospheric Chemistry and Physics* 16.8 (2016): 5229-5241.
- 160 [13] Sandau, Rainer, and Klaus Brieß. "Potential for advancements in remote sensing using small satellites."
161 *The International Archives of the* (2008).
- 162 [14] Williams, Darrel L., Samuel Goward, and Terry Arvidson. "Landsat." *Photogrammetric Engineering*
163 *Remote Sensing* 72.10 (2006): 1171-1178.
- 164 [15] Torres, Ramon, et al. "GMES Sentinel-1 mission." *Remote Sensing of Environment* 120 (2012): 9-24.
- 165 [16] Zhang, Jia-Hua, et al. "Detection, emission estimation and risk prediction of forest fires in China using
166 satellite sensors and simulation models in the past three decades—An overview." *International journal of*
167 *environmental research and public health* 8.8 (2011): 3156-3178.
- 168 [17] Walters, Sandra P., Norma J. Schneider, and John D. Guthrie. "Geospatial Multi-Agency Coordination
169 (GeoMAC) Wildland Fire Perimeters, 2008." *US Geological Survey Data Series* 612.6 (2011).
- 170 [18] Marta, Santa. "Planet Imagery Product Specifications." *Planet Labs*: San Francisco, CA, USA (2018): 91.
- 171 [19] Gesch, Dean, et al. "The national elevation dataset." *Photogrammetric engineering and remote sensing* 68.1
172 (2002): 5-32.
- 173 [20] Glahn, Harry R., and David P. Ruth. "The new digital forecast database of the National Weather Service."
174 *Bulletin of the American Meteorological Society* 84.2 (2003): 195-202.
- 175 [21] Rollins, Matthew G. "LANDFIRE: a nationally consistent vegetation, wildland fire, and fuel assessment."
176 *International Journal of Wildland Fire* 18.3 (2009): 235-249.

177 **Appendix A - Sample of 21 Fires from 2017 Western US Fire Season**

Train Fires

Powerline - ID - Jul	Cove - CA - Jul	Oak - CA - Aug
Swiss Helms - AZ - Jun	Steele - CA - Jul	Indian Ridge - ID - Sep
Creek - CA - Dec	Preacher - NV - Jul	Cub Creek - MT - Sep
Saddle - AZ - Jun	Little Hogback - MT - Aug	Mammoth Cave - ID - Aug
Gutzler - CO - Jul	North Pelican - OR - Aug	Helena - CA - Oct
Sheep - AZ - Jul	Nena Springs - OR - Au	

Test Fires

Pinal - AZ - May
Highline - AZ - June
Sulfur - CA - Oct
Buck - CA - Sept

178 **Appendix B - Details around model hyper parameters for training**

179 The neural network's input was a 3x3 cell array with 11 bands. The first convolutional layer creates 32 filters of
180 the 3x3x11 with a kernel size of 2x2 and the second convolutional layer creates an additional 64 2x2 filters. The
181 third layer is fully connected with 64 neurons followed by a dropout layer of .4. The fourth layer consists of 128
182 fully connected neurons followed by a dropout layer of .2. The fifth, sixth, and seventh/output layers are fully
183 connected with 64, 32, and 1 neurons respectively. The ReLU activation function is used for all layers with the
184 exception of the binary output, which uses a sigmoid function. Binary cross-entropy loss is used with the adam
185 optimizer in both the offline and online setting with epochs, batch size, learning rates (α), and class weights
186 specified below.

187 For offline training, a random sample of one million 3x3x11 images was assembled across all fires. The eleventh
188 band of data representing the then-current state of the fire was substitute with random noise. The model was
189 trained over 300 epochs with a batch size of 40, and a learning rate of $\alpha=1e-5$. Class weights of 1 (no burn) and
190 4 (burn) to account for the uneven distribution of the randomly generated dataset and to maximize recall of the
191 burned area. This approach was thought to be advantaged when moved to the online environment.

192 The agent/model made burn or no burn decisions for each cell and the fire edge over a number of iterations
193 equal to 1.7 times the maximum wind speed. This fixed parameter ν was determined via an independent linear
194 regression of the number of cells burned in a fixed period as a function of the maximum wind speed of the fire,
195 regardless of directional change. For each online session, predictions were initiated as random ($\epsilon=1$) and allowed
196 to become increasingly ϵ -greedy with an exponential decay function where $\lambda=.75$ for each iterative model/agent
197 update.

198 Model/agent updates were performed online after every 10,000 predictions/decisions. The model was trained at
199 each iteration over 80 epochs with a batch size of 400 and a learning rate of $\alpha=1e-3$. Class weights of 1 (no
200 burn) and 2.3 (burn) were used as these values were inversely proportional to their respective frequencies in a
201 random sample of the online training data.

202 **Appendix C - Example of gridded vs smooth RL output**

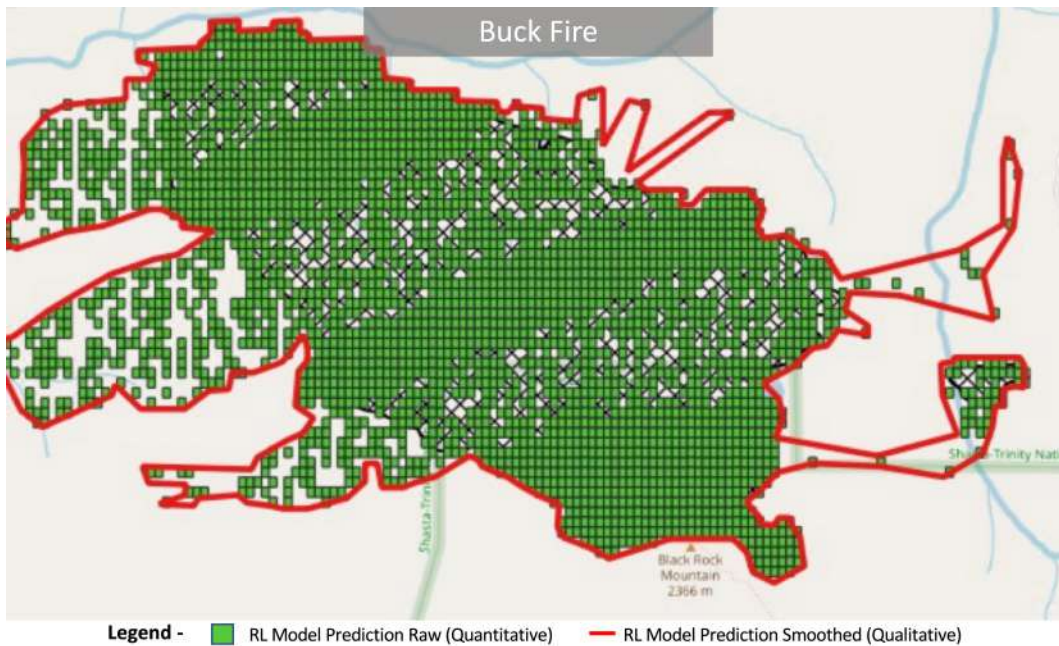


Figure 3: Raw vs Smooothed RL Model Prediction for Buck Fire

203 **Appendix D - Example of RL vs FARSITE on RapidEye imagery**

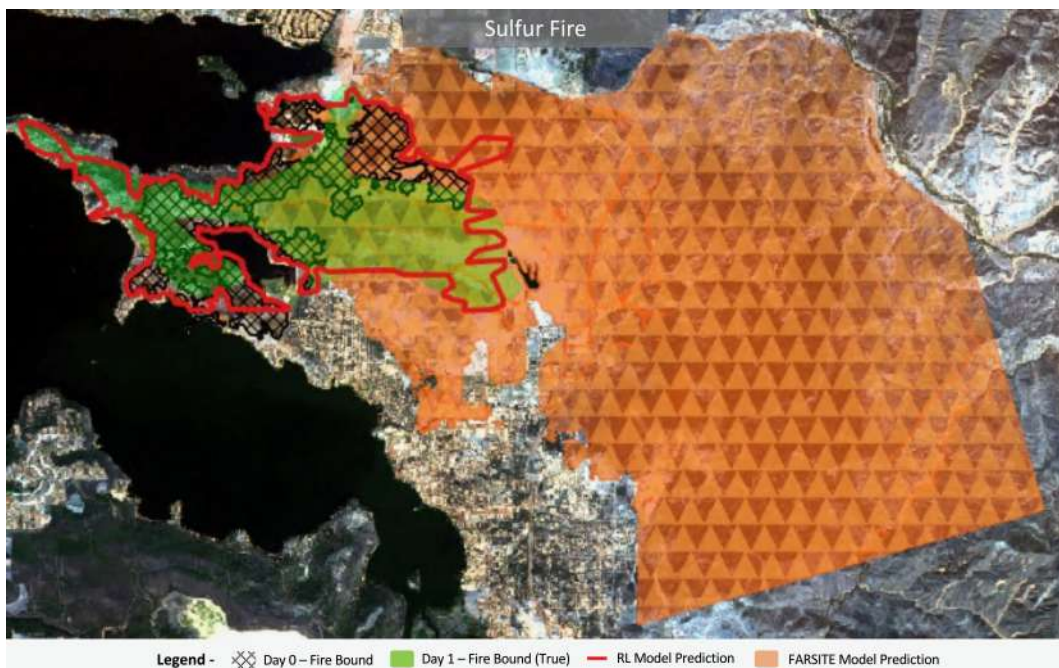


Figure 4: Imagery of site of Sulfur Fire via RapidEye program with RL and FARSITE predictions